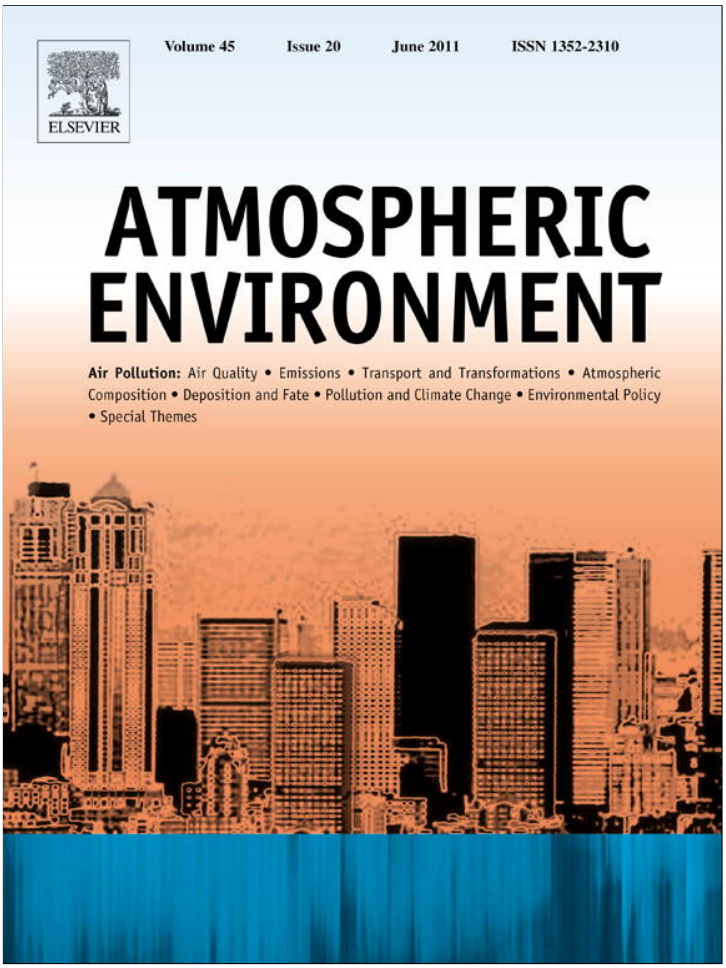

Atmospheric Environment 45 (2011) 3360–3365

Contents lists available at ScienceDirect

Atmospheric Environment

journal homepage: www.elsevier.com/locate/atmosenv

NAO-induced spatial variations of total ozone column over Europe at near-synoptic time scale

Valeriy N. Khokhlov [a,*], Anna V. Romanova [b]

[a] Department of Theoretical Meteorology and Metcasts, Odessa State Environmental University, Lvovskaia str. 15, Odessa 65016, Ukraine
[b] Department of Higher and Applied Mathematics, Odessa State Environmental University, Lvovskaia str. 15, Odessa 65016, Ukraine

ARTICLE INFO

Article history:
Received 30 November 2010
Received in revised form
22 March 2011
Accepted 24 March 2011

Keywords:
North Atlantic Oscillation
Weather pattern
Total ozone column
Wavelet transform

ABSTRACT

The variations of total ozone column over Europe at the multiyear time scale have earlier been characterised by the changes in the phase of North Atlantic Oscillation. Spatial patterns over Europe in total ozone column response to *weather pattern changes* associated with the North Atlantic Oscillation are investigated here using the cross-wavelet transform. The average cross-wavelet powers and local relative phases are calculated. It is shown that near a centre of action associated with the NAO the changes of total ozone column are maximal and become apparent immediately after the changes in the weather pattern.

1. Introduction

When dynamical causes resulting in total ozone column (TOC) variations over some geographical region are considered, at least the two processes are mainly taken into account. Firstly, the TOC varies due to the transport of ozone from other geographical regions. For example, Creilson et al. (2003) showed that the flow regime associated with the positive phase of North Atlantic Oscillation (NAO) causes the transport of ozone from eastern North America across the North Atlantic onto Europe. Also, Auvray and Bey (2005) detected that the contributions from North America and Asia into European total ozone column are comparable. Note that this dynamical process occurs mainly in the troposphere and do not contribute greatly to the column ozone fluctuations. Secondly, the mid-latitude total ozone column varies with the passage of low and high pressure systems, which are associated with a distinct structure near the tropopause; Schubert and Munteanu (1988) showed a correlation between TOC and tropopause variability. Appenzeller et al. (2000) documented a pattern in cross-correlation maps between winter mean tropopause pressure and NAO index. In accordance with their results, during positive NAO phases tropopause pressure is higher at high latitudes and lower at mid-latitudes, as would be expected from an enhanced Icelandic low and Azores high pressure system. Winter mean total ozone is correspondingly reduced at Arosa (at 46.8N, 9.7E; Switzerland) whereas over Iceland total ozone values are enhanced. Brönnimann et al. (2000) and Orsolini and Doblas-Reyes (2003) used long-term records of both atmospheric circulation indices and total ozone. They showed that there exists a strong relation between the total ozone over Europe and the Arctic Oscillation (or NAO) index at monthly and seasonal (winter) time scales.

It is well known (see e.g. Wanner et al., 2001) that the NAO is described by the sea-level pressure seesaw between the subtropical anticyclone near the Azores and the subpolar low pressure system near Iceland. The positive phase of the NAO corresponds to a strong westerly flow and reflects below-normal heights and pressure across the high latitudes of the North Atlantic and above-normal heights and pressure over the central North Atlantic and Western Europe; the opposite pattern occurs during the negative phase of the NAO. In other words, during a month or winter with the positive value of NAO index the Icelandic low and Azores high are mainly located at their conventional places resulting in the above mentioned trends of TOC over Europe. Specifically, the total ozone column over Arosa increases during the winters with negative NAO indices and vice versa.

It should be noted that a large-scale circulation is only one of many factors that affect variations of TOC at intra- and inter-annual time scales; e.g., the solar- and QBO-induced fluctuations of TOC are frequently documented (see e.g. Cordero and Nathan, 2005; Dhomse et al., 2006; Jiang et al., 2008). On the other hand, a few studies only considered the total ozone fluctuations with periods less than the one month (e.g. Orsolini and Limpasuvan, 2001;

* Corresponding author. Tel.: +380 482 326739; fax: +380 482 427767.
E-mail address: vkhokhlov@ukr.net (V.N. Khokhlov).

1352-2310/$ – see front matter © 2011 Elsevier Ltd. All rights reserved.
doi:10.1016/j.atmosenv.2011.03.056

Brönnimann and Hood, 2003; Sych et al., 2005; Ruzmaikin et al., 2007). This scarcity is in addition conditioned by the high level of red noise, which is common for midlatitudes' time series including both TOC and NAO index. Nevertheless, the variations of the NAO index at near-synoptic time scales were documented (Feldstein, 2000; Rivière and Orlanski, 2007), and it is attractive to suppose that there can be some variations of total ozone column caused by the synoptic-scale processes associated with the NAO. However, to our knowledge robust linkages that may imply relationships between the NAO index and total ozone column at near-synoptic time scale have not been established.

This paper is aimed to identify spatial patterns over Europe in total ozone column response to *weather pattern changes* associated with NAO. Here we apply cross-wavelet transform (Grinsted et al., 2004) to a cold-season time series of TOC and NAO index.

2. Data

We examine total ozone time series during nine cold seasons (DJFM) of 1997–2005, measured by the Earth Probe total ozone mapping spectrometer (TOMS V8). A total ozone time series for year *N* refers to December year *N*−1 and January, February, and March year *N*. For example, the 2004 values contain the data of December 2003 and January, February, and March 2004. The data are daily averages on a spatial grid with a 1° × 1.25° (latitude-longitude) cell bounded by the longitudes 15W and 45E and latitudes 35N–60N. The choice of last latitude is conditioned by the missing polar night intervals. The daily total ozone time series are jointly analysing with the daily NAO indices. The Rotated Principal Component Analysis is used to calculate daily NAO indices (see, e.g., Barnston and Livezey, 1987).

It must be noted that Earth Probe TOMS instrument is experiencing calibration problems (e.g. Kiss et al., 2007). The errors are apparently caused by a complex problem involving the instrument's front optics, most likely due to a non-uniform degradation of the scanner mirror. The errors can be as large as 40 DU in total column ozone and become significant beginning mid-2000 when the throughput showed a sharp drop[1]. The resulting ozone is stable within ±1% over the 1996–2005 period, but there is a residual seasonally-dependent error of ±1.5% magnitude during the 2002–2005 in the Northern Hemisphere. Hereupon these data are not recommended to estimate long-term trends. Nevertheless, the use of the data to evaluate some variations during separate cold seasons is, in our opinion, fully justified. Kiss et al. (2007) showed that annual cycles and standard deviations of daily mean total ozone by Nimbus-7 and Earth Probe are fully comparable.

The correlation coefficients between the daily Arosa TOC and NAO index for the nine cold periods are combined into Table 1. It is noteworthy that positive and, moreover, significant correlations between these time series during some years are registered; it is at variance with the findings of Appenzeller et al. (2000) that stated negative correlations. From our data, the correlation coefficient for the cold season of 2002 ($r = -0.53$) only can be matched up the mean correlation ($r = -0.467$) that was documented by Appenzeller et al. (2000). Furthermore, Table 1 misses a relation between the seasonal NAO indices and correlation coefficients. For example, two most negative correlation coefficients occurred both in the case of relatively large NAO index during the cold season of 2002 (NAO index is 0.71, $r = -0.53$) and for the insignificant NAO index in 2002–03 (NAO index is 0.09, $r = -0.32$). It suggests that we can not conclude any relationship between the NAO and TOC variability if daily time series are used.

Table 1
The seasonal (DJFM) NAO indices and correlation coefficients (*r*; significant values are in bold) between the daily NAO index and Arosa TOC.

Year[a]	NAO index[b]	*r*
1997	0.79	0.10
1998	0.02	**0.20**
1999	0.67	−0.15
2000	1.73	**−0.14**
2001	−1.05	−0.04
2002	0.71	**−0.53**
2003	0.09	**−0.32**
2004	−0.10	0.09
2005	0.45	0.20

[a] Here, the DJFM for the individual year starts with 1 December and ends with 31 March (e.g. 1 December 1996 and 31 March 1997) with the exception of years 1998, 1999, and 2004, which start with 13 December, 3 January, and 4 December respectively due to the missing data of total ozone at the start of the cold periods.
[b] The seasonal NAO indices were obtained from www.cgd.ucar.edu/cas/jhurrell/indices.data.html.

Fig. 1 shows the time series of the daily NAO index and Arosa total ozone for the DJFM of 2003–04. First of all, these time series do not display any visible coherence (the correlation coefficient is 0.09 only), which is typical for majority of cold seasons under investigation. Correspondingly, the lack of correlation contradicts to the results of Appenzeller et al. (2000), which can be caused, in our point of view, by the following. First, the daily time series are very noisy, as stated above, and it is no wonder that they are not correlated. Then, a response of total ozone column to changes of tropopause pressure is not instantaneous; hereupon these changes associated with synoptic time scale must appear after some time lags. Finally, Appenzeller et al. (2000) argued negative correlation for monthly Arosa total ozone and NAO index by climatic location of dipole centres associated with the NAO, but anticyclone near the Azores and the low pressure system near Iceland shift frequently from their own distinctive positions during some cold seasons. For example, the NAO negative phase of 2003–04 (see map of rPC1 in Fig. 2) resulted in the low-variable baric field associated with the NAO observed over Arosa; consequently, the NAO does not cause any significant variations of tropopause pressure over that region.

Thus conventional methods, such as correlation analysis or canonical correlation analysis, can not provide satisfactory results. The required method must (i) filter carefully the high-frequency

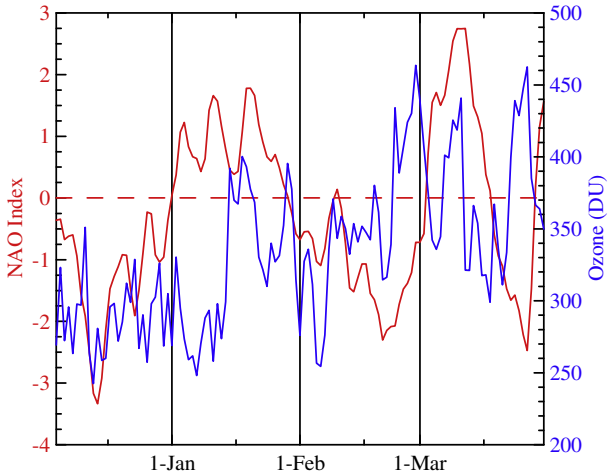

Fig. 1. The daily NAO index and Arosa total ozone (correlation coefficient is 0.09) for DJFM of 2003–04.

[1] McPeters R., Taylor S., Jaross G., Haffner D., Labow G., Kowalewski M., 2007. Empirically corrected TOMS Earth Probe dataset. 17 pp. (http://jwocky.gsfc.nasa.gov/news/Corrected_EP_TOMS_README.pdf).

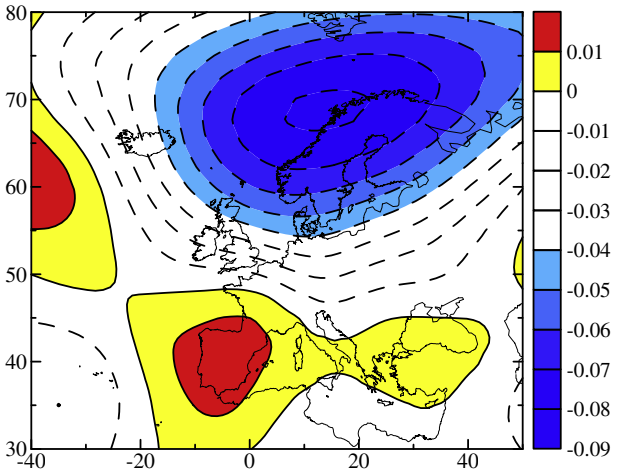

Fig. 2. Spatial distribution of loading of the first rotated principal component (explains 24% of the variance) as a result of PCA from sequential daily 500 hPa geopotential heights during the DJFM of 2003–04. The units are arbitrary.

fluctuations from the time series, but not perturb their statistical stability, and (ii) provide results relating to specific time intervals within the whole period under consideration. In our opinion, the continuous wavelet transform (CWT) meets the above requirements.

3. Methodology

Wavelets are fundamental building block functions, analogous to the trigonometric sine and cosine functions. Fourier transform extracts details from the signal frequency, but all information about the location of a particular frequency within the signal is lost. Wavelet transform expands time series into time-frequency space and can therefore find localized intermittent periodicities. Here, we give only brief details on the continuous wavelet transform (CWT); Torrence and Compo (1998) and Grinsted et al. (2004) have provided more detail survey.

Consider a time series, x_n, with equal time spacing δt and $n = 0 \ldots N-1$, where N is the number of values in the time series. Apply a wavelet function, $\psi_0(\eta)$, as a band-pass filter to the time series. This wavelet function is stretched in time by varying its scale (s), so that $\eta = st$, and normalizing it to have unit energy. The CWT of x_n is defined as the convolution of x_n with a scaled and translated version of wavelet function:

$$W_n^X(s) = \sqrt{\frac{\delta t}{s}} \sum_{n'=0}^{N} x_{n'} \psi_0 \frac{(n'-n)\delta t}{s}. \quad (1)$$

The Morlet wavelet can be chosen as the wavelet function, since it provides a good balance between time and frequency localization (Grinsted et al., 2004). Because the Morlet wavelet is complex, the wavelet transform $W_n^X(s)$ is also complex. Then, the transform can then be divided into the real part, $\Re\{W_n(s)\}$, and imaginary part, $\Im\{W_n(s)\}$, or amplitude, $|W_n(s)|$, and phase, $\tan^{-1}[\Im\{W_n(s)\}/\Re\{W_n(s)\}]$. Finally, we define the wavelet power spectrum as $|W_n(s)|^2$.

The CWT has edge artefacts because the wavelet is not completely localized in time. It is therefore useful to introduce a cone of influence (COI) in which edge effects can not be ignored. The COI is the area in which the wavelet power caused by a discontinuity at the edge has dropped to e^{-2} of the value at the edge.

The statistical significance of wavelet power can be assessed relative to the null hypotheses that the signal is generated by a stationary process with a given background power spectrum. As stated above, an appropriate background signal is red noise, and its power spectrum is used to establish a null hypothesis for the significance of a peak in the wavelet power spectrum (Torrence and Compo, 1998).

The cross-wavelet transform (XWT) of two time series x_n and y_n is defined as $W^{XY} = W^X W^{Y*}$, where the asterisk denotes complex conjugation. Then, the cross-wavelet power is defined as $|W^{XY}|$, and the complex argument $\arg(W^{XY})$ is the local relative phase between x_n and y_n in time-frequency space. Confidence levels for the cross-wavelet power can be also derived (Torrence and Compo, 1998).

It is apparently that a lot of work and a long time are necessary to consider visually more than one thousand (the total number of grid points is 1274) figures with patterns of XWT, and this way is not optimal. Thus in this study we are working with the XWT in the following way:

(i) the XWT is performed for each grid point within the longitudes from 15W to 45E and latitudes from 35N to 60N;
(ii) within the areas in the time-frequency domain, where the cross-wavelet power is above the 5% significance level, the average cross-wavelet power is calculated for each grid points;
(iii) within the same areas, the local relative phase is converted into the time lag (this procedure is easy as the period for each scale is known), and the average time lag is calculated for each grid points;
(iv) finally, these average values are plotted on the geographical map, and such spatial distributions are analyzed in the next section.

Let us notice that wavelet transform had been used to analyse temporal variations of total ozone, e.g. Glushkov et al. (2005), Borchi et al. (2006), but another version of transform named the non-decimated wavelet transform or multi-resolution analysis was applied.

4. Results and discussion

First, the CWT of the daily NAO index and Arosa total ozone during the cold season of 2003–04 are shown in Figs. 3 and 4.

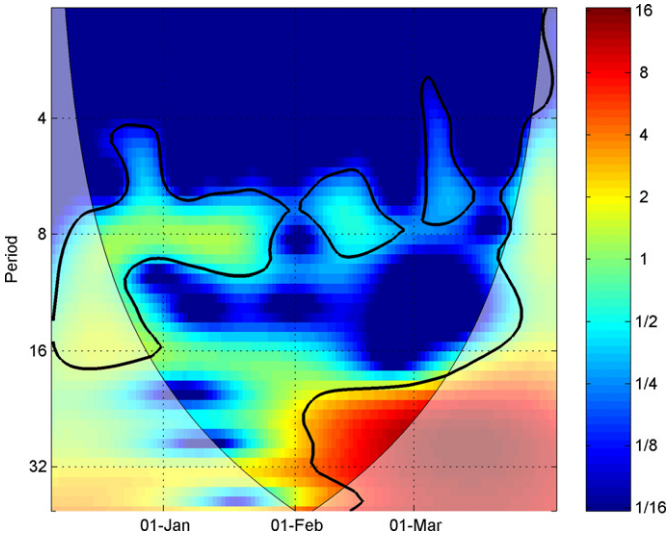

Fig. 3. Continuous wavelet power spectrum of daily NAO index for DJFM of 2003–04. The colour scale represents the wavelet power in arbitrary units. The thick black contour designates the 5% significance level against red noise and the cone of influence, where edge effects might distort the picture, is shown as a lighter shade.

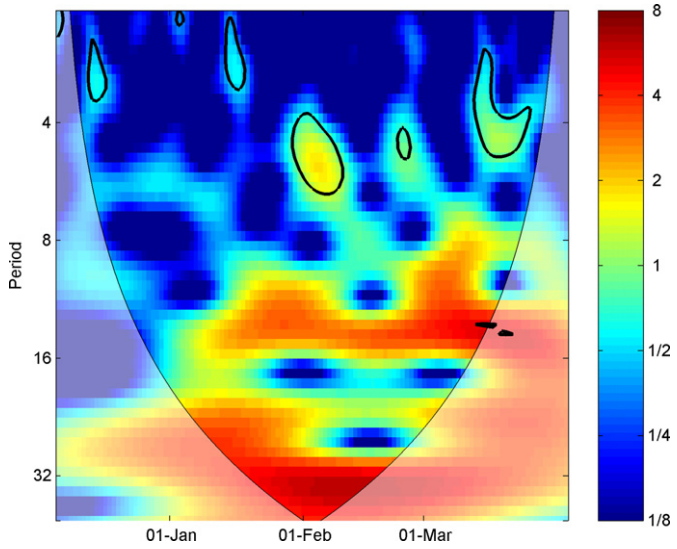

Fig. 4. As in Fig. 3 but for daily Arosa total ozone.

Outside the cone of influence, the daily NAO index has the significant peaks of the wavelet power in the ~8 day band during almost whole cold period; this peak is most prominent in December 2003 and January 2004. On the other hand, the majority of significant peaks obtained by the CWT of daily Arosa total ozone occur in the band with periods lesser 8 days. Other striking feature is the mismatch observed for the maxima of the wavelet power in the 8–16 day band: when the wavelet power of daily NAO index is maximal, for the Arosa total ozone the power is minimal, and vice versa. Thus the similarity between the patterns shown in Figs. 3 and 4 is quite low and it is hard to establish any relations between the two time series.

Next, Fig. 5 shows the XWT of the daily NAO index and Arosa total ozone for DJFM of 2003–04. It is noteworthy that there is cross-wavelet power of the time series that is significant at the 5% level. This significant common power is observed in the ~8 day band during ~15 day intervals in the January, February and March. Here we must note that this feature is common for the overwhelming majority of grid points, so it can be to some extent considered as natural phenomenon describing the influence of the NAO on the total ozone column variability at this time scale. It is also noteworthy that in January, when the positive phase of NAO was observed (see Fig. 1), the variations of the NAO index are leading the Arosa total ozone with time lag ~4 days, whereas when the negative phase predominated in February the NAO index and Arosa total ozone were mainly in-phase. Thus we can speculate that the filtering of high-frequency fluctuations, which was provided by CWT, allows extracting the features from the daily time series like those were obtained using monthly time series.

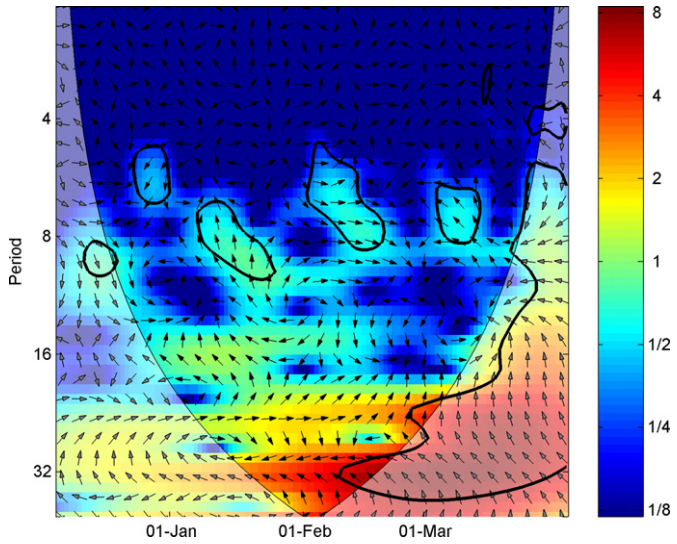

Fig. 5. Cross wavelet transform of the time series from Fig. 1. The colour scale represents the cross-wavelet power in arbitrary units. The 5% significance level against red noise is shown as a thick contour. The relative phase relationship is shown as arrows with in-phase pointing right, anti-phase pointing left, and the NAO index leading the Arosa TOC.

Same features are distinctive for all cold seasons of 1996–2005, i.e. are not unique for the DJFM of 2003–04 only. Table 2 shows dates during individual cold seasons, when significant cross-wavelet powers were obtained at some time scales. Really, such time scales are near-synoptic over the range 4–8 days, and the durations of period with the significant powers are commonly two weeks. However, the time lags, calculated from the mean phase angles, are in the range 0–6 days, i.e. a response of the Arosa total ozone to some event related to the NAO differs occasionally. Though it can be noted one regularity – variations of daily TOC and NAO index are out of phase in the case of sufficiently large positive NAO indices (absolute values of mean phase angles are close to 180° in 1997, 2000, 2003, and 2005) – it is difficult to conclude unambiguously an effect of the NAO on the total ozone column at synoptic time scale. In our opinion, the spatial diversity of baric field (as well as other meteorological fields) relating to the North Atlantic Oscillation have an impact here; thereupon we must take into account both time and spatial variability at the synoptic scale.

Finally, an analysis of total ozone's spatial variations would be carried out jointly with some measure describing weather pattern changes; we use here the maps of first rPC1 for 500 hPa geopotential heights calculated for January and February 2004 when the significant cross-wavelet powers are observed. These maps represent well enough the alternation of the NAO phases. For example, the positive NAO phase occurs dominantly during January 2003 (see Fig. 1), and the rPC1 in Figs. 6a and 7a is determined by the dipole with the negative anomaly near Iceland and the positive one over Western Mediterranean; on the contrary, when the negative NAO phase is observed in February 2004 the negative anomaly of above dipole shifts towards Scandinavia (Figs. 6b and 7b), and this, in fact, explains the negative NAO phase.

Spatial distributions of average time lags and cross-wavelet powers (Figs. 6 and 7) suggest the validity of our choice. Indeed,

Table 2
The dates and typical time scales, when significant common wavelet powers during individual years were registered for the daily NAO index and Arosa TOC. Mean phase angles and time lags are calculated using data within areas with significant common wavelet powers, and NAO indices are averaged out for these dates.

Year	Date[a]	Time scale (days)[a]	Mean phase angle (degrees)[b]	Time lags (days)	NAO indices
1997	10 Feb–10 Mar	5–6	−150	2.5	1.28
1998	01 Jan–15 Jan	6–8	67	5.2	0.59
1999	20 Feb–05 Mar	5–7.5	27	6.3	0.63
2000	05 Feb–25 Feb	5–7	179	3.0	1.30
2001	25 Dec–15 Jan	4–6	−16	0.3	−0.29
2002	10 Feb–20 Feb	6.5–8	90	5.3	0.72
2003	01 Feb–20 Feb	4.5–7	−145	2.7	0.70
2004	05 Feb–20 Feb	5–8	−2	0.0	0.41
2005	10 Jan–25 Jan	5–7.5	−142	3.1	0.80

[a] Dates and time scales are given approximately because the areas with significant values of cross-wavelet power are outlined by irregular curves not rectangles (e.g. see Fig. 5).

[b] Circular mean of phase angles is calculated following to Grinsted et al. (2004).

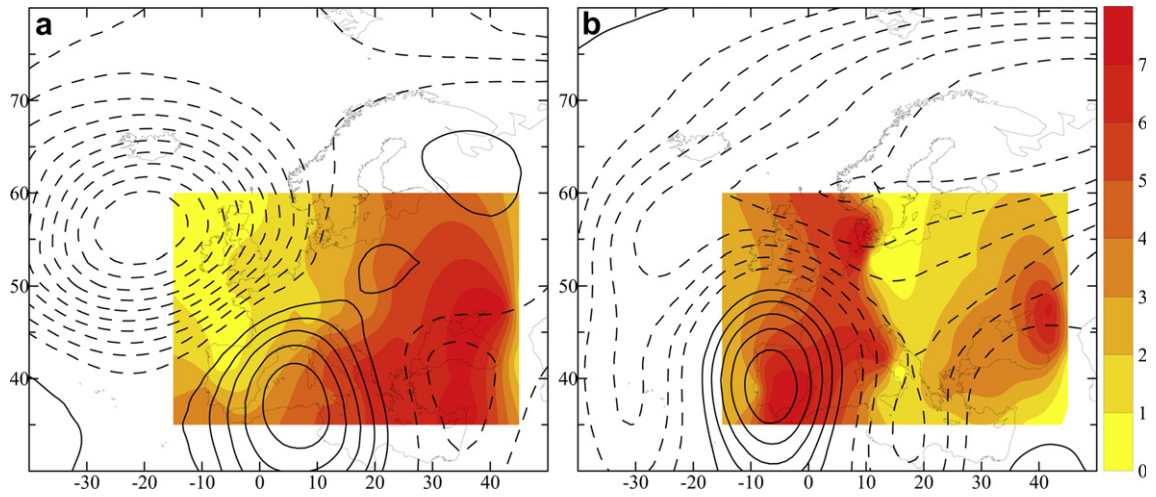

Fig. 6. Spatial distributions of time lags (days) for response of total ozone to changes of NAO in the ~8 day band in (a) January and (b) February 2004. The colour scale represents the time lags (days). The time lags were averaged within the areas in the time-frequency domain, where the cross-wavelet power is above the 5% significance level. The map of rPC1 (black lines) for 500 hPa geopotential heights (solid lines – positive, dashed lines – negative) are shown for (a, explains 37% of variance) January and (b, explains 32% of variance) February 2004.

features of spatial distribution for the local time lags in total ozone variation response onto NAO index changes coincide generally with weather pattern variability. In January, closer to the main anomaly in the North Atlantic the total ozone column varies almost coherently with the baric field (time lag is up to 2 days); as this anomaly is farther, the time lag increases and amounts to approximately 8 days in Eastern Mediterranean and Black Sea (Fig. 6a). In February, this pattern is same, and the peculiar "trough" spreading from Baltic Sea to Central Mediterranean is its interesting feature (Fig. 6b). A perfect coincidence can not be certainly observed; it must be however noted that the variability of baric field is analyzed using only the first component of decomposition by the principal component analysis. Spatial distribution of cross-wavelet power obeys the above mentioned pattern – its maxima occur nearby the main negative anomaly associated with the NAO, and its minima have place within the anomaly with the opposite sign (Fig. 7). Summarizing, the results in Figs. 6 and 7 correspond generally to those of Appenzeller et al. (2000) except that our results describe the variability at the time scale of approximately 8 days. Therefore, the variability of total ozone column can be explained by the variability of synoptic processes.

The conclusion in the last sentence is not new. For example, Kulkarni et al. (2011) have showed the high concentration of tropospheric ozone in July over the Atlantic Ocean near Iberian Peninsula is due to the presence of Azores anticyclone. During the past two decades many researchers [see e.g. Orsolini et al. (1998), Bojkov and Balis (2001), Orsolini and Limpasuvan (2001), Barriopedro et al. (2010)] have studied an influence of cyclones and anticyclones on total ozone variation over North Atlantic and Europe; main outcome consists in that the synoptic activity can result in the appearance of ozone miniholes. On the one hand, the ozone miniholes arise from the transport of low-latitude, ozone-poor air into Europe, which can be observed during strong positive phase of the NAO. During the NAO's positive phases the main storm tracks shift northward and contribute to the intrusion of ozone-poor air from south. On the other hand, Barriopedro et al. (2010) showed that the minihole frequency during cold period correlates with blocking frequency. If take into account the assumption putted forward by Stein (2000) that blocking activity intensifies during weak NAO events, such an explanation mismatches in many respects with the stated above.

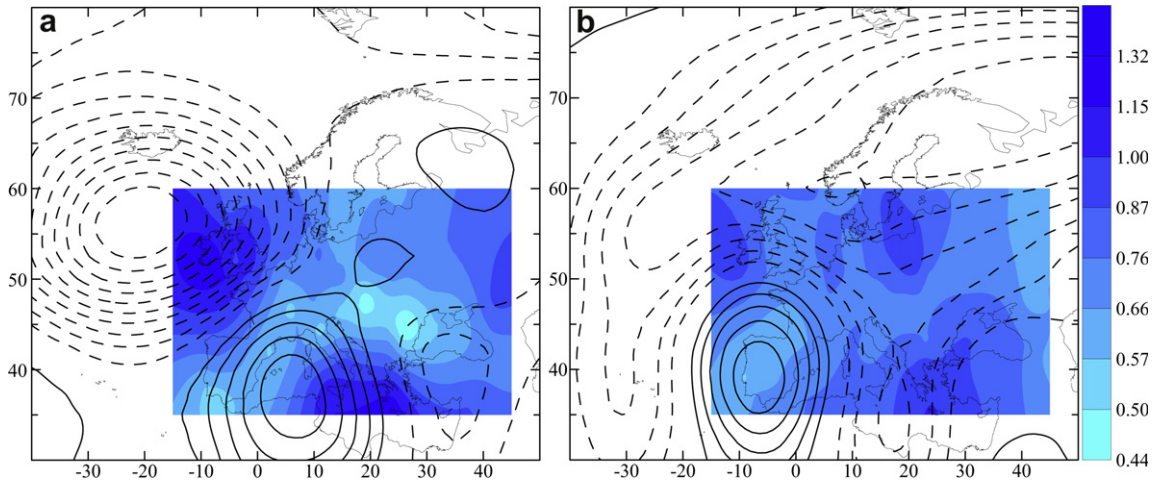

Fig. 7. As in Fig. 6 but for spatial distributions of cross-wavelet power of total ozone and NAO index. The colour scale represents the cross-wavelet power in arbitrary units.

Our results show that the spatiotemporal variations of TOC over Europe due to the NAO-induced cyclonic/anticyclonic activity much differ from one case to other one, and the NAO influences the TOC both in the positive and weak phases (see Table 2). However the phase NAO defines the tracks (or persistent locations) of cyclones and anticyclones during two or three weeks, which can cause the appearance of minihole in any part of Atlantic-European region.

5. Conclusions

The cross-wavelet transform is applied to the daily time series of total ozone column over Europe and NAO index and found to be useful for making conclusions on coherent variability for these time series at the temporal and spatial scales defining weather pattern. It is noteworthy that such variability occurs at the near-synoptic time scales typical for the NAO (see, e.g. Feldstein, 2000; Rivière and Orlanski, 2007).

Most prominent feature is that local time lags for variability of the total ozone column over Europe depend, in some way, on the distance from the centre of action associated with the NAO, and the cross-wavelet power is determined by a sign of pressure anomaly in the main centre of action in North Atlantic. In our opinion, the results here detect the primary importance of the North Atlantic Oscillation in the spatiotemporal variability of the total ozone column over Europe.

Acknowledgements

The expert comments by two anonymous reviewers have markedly improved the quality of this manuscript and we thank them. Some preliminary outcomes were presented at the 4th SPARC General Assembly (Bologna, Italy, September 2008). Cross-wavelet software was provided by A. Grinsted (Arctic Centre, University of Lapland, Rovaniemi, Finland). The authors thank the National Space Science Data Centre at NASA, USA for providing TOMS ozone data.

References

Appenzeller, C., Weiss, A.K., Staehelin, J., 2000. North Atlantic Oscillation modulates total zone winter trends. Geophysical Research Letters 27, 1131–1134.

Auvray, M., Bey, I., 2005. Long-range transport to Europe: seasonal variations and implications for the European ozone budget. Journal of Geophysical Research 110, D11303. doi:10.1029/2004JD005503.

Barnston, A.G., Livezey, R.E., 1987. Classification, seasonality and persistence of low-frequency atmospheric circulation patterns. Monthly Weather Review 115, 1083–1126.

Barriopedro, D., Antón, M., García, J.A., 2010. Atmospheric blocking signatures in total ozone and ozone miniholes. Journal of Climate 23, 3967–3983. doi:10.1175/2010JCLI3508.1.

Bojkov, R.D., Balis, D.S., 2001. Characteristics of episodes with extremely low ozone values in the northern middle latitudes 1957–2000. Annales Geophysicae 19, 797–807.

Borchi, F., Naveau, P., Keckhut, P., Hauchecorne, A., 2006. Detecting variability changes in Arctic total ozone column. Journal of Atmospheric and Solar-Terrestrial Physics 68, 1383–1395. doi:10.1016/j.jastp.2006.05.011.

Brönnimann, S., Hood, L.L., 2003. Frequency of low-ozone events over northwestern Europe in 1952–1963 and 1990–2000. Geophysical Research Letters 30, 2118. doi:10.1029/2003GL018431.

Brönnimann, S., Luterbacher, J., Schmutz, C., Wanner, H., Staehelin, J., 2000. Variability of total ozone at Arosa, Switzerland, since 1931 related to atmospheric circulation indices. Geophysical Research Letters 27, 2213–2216.

Cordero, E.C., Nathan, T.R., 2005. A new pathway for communicating the 11-year solar cycle signal to the QBO. Geophysical Research Letters 32, L18805. doi:10.1029/2005GL023696.

Creilson, J.K., Fishman, J., Wozniak, A.E., 2003. Intercontinental transport of tropospheric ozone: a study of its seasonal variability across the North Atlantic utilizing tropospheric ozone residuals and its relationship to the North Atlantic Oscillation. Atmospheric Chemistry and Physics 3, 2053–2066.

Dhomse, S., Weber, M., Wohltmann, I., Rex, M., Burrows, J.P., 2006. On the possible causes of recent increases in northern hemispheric total ozone from a statistical analysis of satellite data from 1979 to 2003. Atmospheric Chemistry and Physics 6, 1165–1180.

Feldstein, S.B., 2000. The timescale, power spectra, and climate noise properties of teleconnection patterns. Journal of Climate 13, 4430–4440.

Glushkov, A.V., Khokhlov, V.N., Loboda, N.S., 2005. Influence of the Antarctic Oscillation on the total ozone content in the Southern Hemisphere. In: van Amstel, A. (Ed.), Non-CO_2 Greenhouse Gases: Science, Control, Policy and Implementation. Millpress, Rotterdam, pp. 297–304.

Grinsted, A., Moore, J.C., Jevrejeva, S., 2004. Application of the cross wavelet transform and wavelet coherence to geophysical time series. Nonlinear Processes in Geophysics 11, 561–566.

Jiang, X., Pawson, S., Camp, C.D., Nielsen, J.E., Shia, R.-L., Liao, T., Limpasuvan, V., Yung, Y.L., 2008. Interannual variability and trends of extratropical ozone. Part I: Northern Hemisphere. Journal of the Atmospheric Sciences 65, 3013–3029. doi:10.1175/2008JAS2665.1.

Kiss, P., Jánosi, I.M., Torres, O., 2007. Early calibration problems detected in TOMS Earth-probe aerosol signal. Geophysical Research Letters 34, L07803. doi:10.1029/2006GL028108.

Kulkarni, P.S., Bortoli, D., Salgado, R., Antón, M., Costa, M.J., Silva, A.M., 2011. Tropospheric ozone variability over the Iberian Peninsula. Atmospheric Environment 45, 174–182. doi:10.1016/j.atmosenv.2010.09.029.

Orsolini, Y.J., Doblas-Reyes, F.J., 2003. Ozone signatures of climate patterns over the Euro-Atlantic sector in the spring. Quarterly Journal of the Royal Meteorological Society 129, 3251–3263. doi:10.1256/qj.02.165.

Orsolini, Y.J., Limpasuvan, V., 2001. The North Atlantic Oscillation and the occurrences of ozone miniholes. Geophysical Research Letters 28, 4099–4102.

Orsolini, Y.J., Stephenson, D.B., Doblas-Reyes, F.J., 1998. Storm track signature in total ozone during northern hemisphere winter. Geophysical Research Letters 25, 2413–2416.

Rivière, G., Orlanski, I., 2007. Characteristics of the Atlantic storm-track eddy activity and its relation with the North Atlantic Oscillation. Journal of the Atmospheric Sciences 64, 241–266. doi:10.1175/JAS3850.1.

Ruzmaikin, A., Santee, M.L., Schwartz, M.J., Froidevaux, L., Pickett, H., 2007. The 27-day variations in stratospheric ozone and temperature: new MLS data. Geophysical Research Letters 34, L02819. doi:10.1029/2006GL028419.

Schubert, S.D., Munteanu, M.-J., 1988. An analysis of tropopause pressure and total ozone correlations. Monthly Weather Review 116, 569–582.

Stein, O., 2000. The variability of Atlantic-European blocking as derived from long SLP time series. Tellus 52A, 225–236.

Sych, R.A., Matafonov, G.K., Belinskaya, A.Ju., Ferreira, N.J., 2005. The periodic spatial-temporal characteristics variations of the total ozone content. Journal of Atmospheric and Solar-Terrestrial Physics 67, 1779–1785. doi:10.1016/j.jastp.2005.03.011.

Torrence, C., Compo, G.P., 1998. A practical guide to wavelet analysis. Bulletin of the American Meteorological Society 79, 61–78.

Wanner, H., Brönnimann, S., Casty, C., Gyalistras, D., Luterbacher, J., Schmutz, C., Stephenson, D., Xoplaki, E., 2001. North Atlantic Oscillation – concepts and studies. Surveys of Geophysics 22, 321–382.